Vostok (Antarctica) ice-core time-scale from datings of different origins

Andrey N. Salamatin, Elena A. Tsyganova, Vladimir Y. Lipenkov, Jean-Robert Petit

Vostok (Antarctica) ice-core time-scale from datings of different origins

Andrey N. SALAMATIN,[1] Elena A. TSYGANOVA,[1] Vladimir Ya. LIPENKOV,[2] Jean Robert PETIT[3]

[1]*Department of Applied Mathematics, Kazan State University, 420008 Kazan, Russia*
E-mail: Andrey.Salamatin@ksu.ru
[2]*Arctic and Antarctic Research Institute, 199397 St Petersburg, Russia*
[3]*Laboratoire de Glaciologie et Géophysique de l'Environnement du CNRS, 54 rue Molière, BP 96, 38402 Saint-Martin-d'Hères Cedex, France*

ABSTRACT. Three different approaches to ice-core age dating are employed to develop a depth–age relationship at Vostok, Antarctica: (1) correlating the ice-core isotope record to the geophysical metronome (Milankovich surface temperature cycles) inferred from the borehole temperature profile, (2) importing a known chronology from another (Devils Hole, Nevada, USA) paleoclimatic signal, and (3) direct ice-sheet flow modeling. Inverse Monte Carlo sampling is used to constrain the accumulation-rate reconstruction and ice-flow simulations in order to find the best-fit glaciological time-scale matched with the two other chronologies. The general uncertainty of the different age estimates varies from 2 to 6 kyr on average and reaches 6–15 kyr at maximum. Whatever the causes of this discrepancy might be, they are thought to be of different origins, and the age errors are assumed statistically independent. Thus, the average time-scale for the Vostok ice core down to 3350 m depth is deduced consistent with all three dating procedures within the standard deviation limits of ±3.6 kyr, and its accuracy is estimated as 2.2 kyr on average. The constrained ice-sheet flow model allows, at least theoretically, extrapolation of the ice age–depth curve further to the boundary with the accreted lake ice where (at 3530 m depth) the glacier-ice age may reach ∼2000 kyr.

1. INTRODUCTION

Ice age-dating is one of the principal steps in ice-core data interpretations and paleoclimatic reconstructions. There is no universal and/or standard procedure to determine depth–age relationships in polar ice sheets at deep-drilling sites. The latter question is of primary importance for the record 3600 m deep ice core retrieved from the Antarctic ice sheet at Vostok station (Petit and others, 1999) above the vast subglacial lake.

Applicability of sophisticated two- and three-dimensional (2-D and 3-D) thermomechanical ice-flow models (Ritz, 1992; Ritz and others, 2001) for solving this problem suffers significantly from uncertainties in initial and input data: mainly in glacier bottom conditions and past accumulation rates. Nevertheless, the detailed analysis by Parrenin and others (2001) shows that the modeling of ice-sheet dynamics becomes a useful tool for ice age prediction if a priori chronological information is used to fit the model parameters. Although different sources of age markers and dated time series have their own specific errors, they may be considered reliable constraints if, in combination, they deliver statistically valid and independent estimates of ice age at various depth levels. The inverse Monte Carlo sampling method (e.g. Mosegaard and Tarantola, 1995; Mosegaard, 1998) is especially helpful in this case (Parrenin and others, 2001) to fit the ice-sheet model on average, uniformly vs depth, although without putting excess weight on local fluctuations of the simulated depth–age curve caused by uncertainties in environmental conditions, reconstructed ice accumulation and other paleoclimatic characteristics. From this point of view, even simplified ice-flow models (e.g. Salamatin and Ritz, 1996; Hondoh and others, 2002) may be appropriate for incorporating the principal laws of ice-sheet dynamics into the ice-core dating procedure.

Among different depth–age relationships developed for Vostok, the geophysical metronome time-scale (GMTS), extended in Salamatin and others (1998a) and Salamatin (2000) to the maximum depth 3350 m of the Vostok ice-core isotope record covering four interglaciations, represents the so-called orbitally tuned chronologies. It is based on correlation of the isotopic temperature signal with the geophysical-metronome Milankovich components of past local surface temperature variations inferred from the borehole temperature profile. Possible errors and uncertainties in GMTS are discussed elsewhere (Salamatin and others, 1998b; Salamatin, 2000), and its overall average accuracy was estimated as ±3.5–4.5 kyr. Orbital ice-age control points used in Parrenin and others (2001) as model constraints coincide (to within ±2 kyr) with the corresponding GMTS ages.

Another paleotemperature proxy signal spanning >500 000 years is available from the calcite core (DH-11) in Devils Hole, Nevada, U.S.A. (Winograd and others, 1992, 1997). The principal advantage of this $\delta^{18}O$ record is that the dense vein calcite provides material for direct uranium-series dating (Ludwig and others, 1992), with the standard errors increasing from 1 to 7 kyr with time up to 400 kyr BP. In addition, the signal may be influenced by different hydrological factors. In particular, a systematic underestimation of the ages determined, on the order of several thousands of years, may take place due to the groundwater travel time through the aquifer (Winograd and others, 1992; Landwehr and Winograd, 2001). Nevertheless, the correlation of the Vostok ice-core deuterium–depth signal with the Devils

Hole record (see US Geological Survey open-file report 97-792 at http://pubs.water.usgs.gov/ofr97–792) can also be considered as an independent approach to dating the longest paleoclimate archive from central Antarctica (Landwehr and Winograd, 2001).

The possibility of using various gas studies of Vostok ice cores for relative dating (correlation) with other Antarctic, Greenland or deep-sea core climatic records is not considered here, because of the additional errors which arise from the uncertainty in the gas–ice age difference, preventing better constraints on the ice age. These questions are addressed by Salamatin and others (1998b) and with a deeper focus by Parrenin and others (2001).

Thus, the principal goals of our study are (1) to combine the above sources of chronological information in order to constrain ice-flow model parameters, reducing to a minimum systematic errors in the glaciological time-scale based on simulations of the ice-sheet dynamics in the vicinity of Vostok station, (2) to deduce the average age–depth relationship consistent with different approaches to the ice-core dating within the upper 3350 m, and (3) to extend the model predictions at Vostok to the deeper bottom part of the glacier.

2. MODEL DESCRIPTION AND PARAMETERIZATION

Here we use a simplified 2-D approach to ice flowline modeling developed for ice age predictions by Hondoh and others (2002). We introduce the longitudinal coordinate s as a distance from the ice divide along a reference flowline. The flow tube configuration is described by its relative width $H(s)$ and the ice equivalent thickness $\Delta(s,t)$ depending on time t. The vertical coordinate ζ is the relative distance from the glacier bottom expressed in equivalent thickness of pure ice and normalized by Δ. The paleoclimate is characterized by the surface ice mass balance $b(s,t)$.

An ice-particle trajectory passing through a given point (s_0,ζ_0) can be approximated as

$$\frac{\zeta_0}{\zeta}\approx\frac{\int_0^{s_0}\overline{b}H\mathrm{d}s}{\int_0^{s}\overline{b}H\mathrm{d}s}, \qquad (1)$$

where $\overline{b}(s)$ is the normalized spatial distribution of the accumulation rate along the flowline. Observations by Siegert and others (2001), Bell and others (2002) and preliminary temperature simulations indicate that the basal melting is not likely to occur along the Vostok flowline, and its influence on the ice-sheet dynamics is neglected.

Temporal variations of b and Δ are described in the following parametric form:

$$b=b_0\overline{b}(s)\exp\left(\eta_\mathrm{b}\frac{\delta\mathrm{D}-8\delta^{18}\mathrm{O}_\mathrm{sw}}{C_\mathrm{T}}\right),$$

$$\Delta=\Delta_0(s)+\delta\Delta(t). \qquad (2)$$

Here b_0 is the present-day ice mass balance at the site under consideration ($s=s_0$), and $\Delta_0(s)$ is the present-day glacier thickness (in ice equivalent) along the flowline. The last exponential term in the first of Equations (2) describes the past changes in precipitation traditionally correlated to the inversion (isotopic) temperature in accordance with Robin (1977) and Ritz (1989, 1992). The accumulation-rate variations in central Antarctica are linked by means of the exponential factor η_b and the deuterium/inversion-temperature slope C_T to the ice-core isotopic content ratios δD corrected for past changes in the oxygen isotope composition of ocean water $\delta^{18}\mathrm{O}_\mathrm{sw}$ (Sowers and others, 1993; Bassinot and others 1994). Deviations δD and $\delta^{18}\mathrm{O}_\mathrm{sw}$ in Equations (2) are referenced to their present-day values. For relatively small ratio $\eta_\mathrm{b}/C_\mathrm{T}$ the accumulation-rate variations become linearly dependent on isotopic temperatures. A more sophisticated relationship between the inversion temperature and the deuterium content in ice, directly taking into account the water-vapor source temperature variations, has recently been suggested by Cuffey and Vimeux (2001). Correspondingly, as emphasized and explained by Jouzel and others (2003), the correction of δD to the sea-water isotopic content $\delta^{18}\mathrm{O}_\mathrm{sw}$ enters the transfer function with the factor of 4.8 rather than 8 (used here for consistency with the earlier studies). As shown below in section 4, this leads to slight overestimation of the isotope/temperature gradient C_T.

Ice-sheet thickness fluctuations $\delta\Delta(t)$ in the second of Equations (2) are reconstructed after Salamatin and Ritz (1996). The latter model for $\delta\Delta$ was verified and its tuning parameters γ_b and γ_I were constrained on the basis of the 2-D thermomechanically coupled model of Antarctic ice-sheet dynamics (Ritz, 1992). These results have also been recently supported by 3-D simulations (Ritz and others, 2001). As follows from Salamatin and Ritz (1996), γ_I is inversely proportional to the modified Glen flow-law exponent β, which takes account of the vertical temperature gradient (Lliboutry, 1979). It decreases from 2.5 to 2.1 when β increases from 10 to 20; γ_b can be fixed as 0.56.

The ice-particle motion in the vertical direction is predicted (Hondoh and others, 2002) from an ordinary differential equation with respect to $\zeta=\zeta(t)$

$$\frac{\mathrm{d}\zeta}{\mathrm{d}t}=-\frac{b}{\Delta}\left\{\zeta-\frac{\sigma}{\beta+1}(1-\zeta)\left[1-(1-\zeta)^{\beta+1}\right]\right\} \qquad (3)$$

with b, Δ and s related to ζ and t by Equations (1) and (2). By definition, σ is the proportion of the total ice-flow rate through the reference flow tube due to plastic (shear) deformation of the glacier body, $0\le\sigma\le1$.

Finally, the ice age t_0 of the ζ_0 level at $s=s_0$ is determined by equality $\zeta(t_0)=\zeta_0$, where $\zeta(t)$ is the solution of Equation (3) at the initial condition $\zeta|_{t=0}=1$. A depth–age relationship used initially for the ice-core deuterium record in Equations (2) is corrected through iterative modeling.

The ζ coordinate is expressed via depth h (after Salamatin, 2000) as:

$$\zeta=1-\frac{h}{\Delta}+\frac{c_\mathrm{s}}{\gamma_\mathrm{s}\Delta}\left(1-\mathrm{e}^{-\gamma_\mathrm{s}h}\right), \qquad (4)$$

where C_s is the surface snow porosity and γ_s the exponential densification factor.

Although computation of the depth–age relation is finally reduced to solving a 'one-dimensional' Equation (3), the dating procedure itself is originally based on a 2-D ice-flow model, and thus inherits the principal laws of ice-sheet dynamics, taking into account the geographic conditions and climate changes. One might argue (Hondoh and others, 2002) that such a simple approach to ice age prediction is rather rough and includes several tuning parameters. However, even much more complicated 2-D or 3-D models

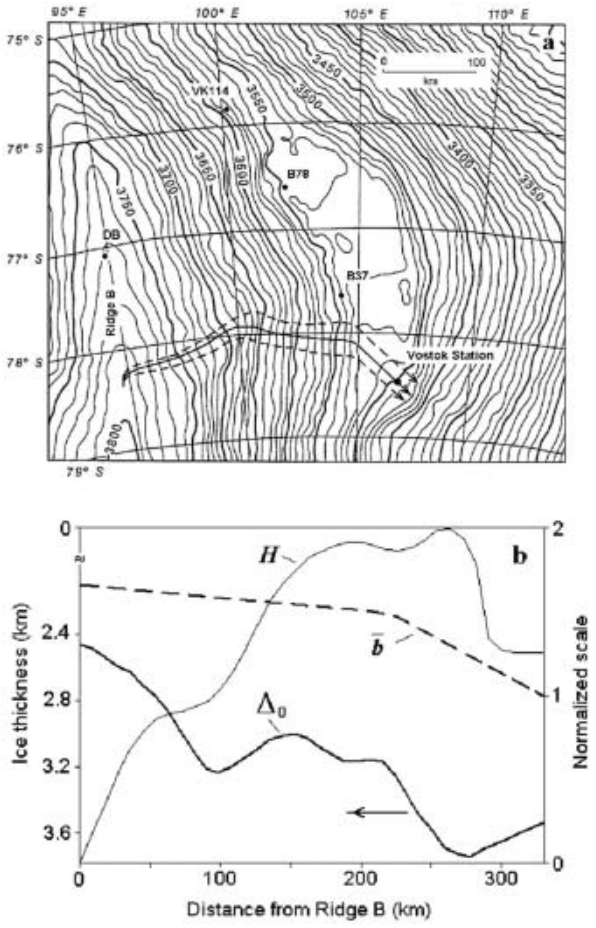

Fig. 1. Geographic conditions around Vostok station. (a) A schematic map of the Vostok lake vicinities adapted after Siegert and Ridley (1998) and the Vostok flowline considered in the ice age simulations (see text). (b) The present-day ice-sheet thickness Δ_0 together with the relative ice-flow tube width H and normalized accumulation rate $\bar{b}$ vs distance measured from Ridge B along the reference flowline in (a).

Table 1. Ice-flow model parameters for Vostok area

Definition of parameter	Denotation	Value
Snow–firn densification and mass balance		
Surface snow porosity	c_s	0.69
Exponential densification factor (m^{-1})	γ_s	0.021
Present-day ice accumulation rate at Vostok ($cm\,a^{-1}$) †	b_0	2.15–2.4
Paleoclimatic exponential factor ($°C^{-1}$)	η_b	0.11
Deuterium/inversion-temperature slope ($‰\,°C^{-1}$) †	C_T	6.0 ± 3.0
Ice-flow conditions		
Distance from ice divide (Ridge B) (km)	s_0	330
Glen flow-law exponent	α	3.0
Modified Glen flow-law exponent	β	10–20
Shear-flow rate factor	σ	0, $s_0 > s > s_l$; σ_l, $s_l > s > s_h$; 0.7–1.0, $s_h > s > 0$
Parameter σ in the intermediate flow zone†	σ_l	0–1
Ice-sheet grounding line at Vostok lake (km) †	s_l	275 ± 30
Ridge B highlands boundary (km) †	s_h	20–80
Model of ice-sheet thickness variations (Salamatin and Ritz, 1996)		
Spatial mass-balance amplification factor	γ_b	0.56
Ice-sheet growth feedback factor	γ_l	2.5–2.1

† Parameters estimated through model constraining by Monte Carlo sampling method.

cannot resolve the uncertainties about ice-deformation mechanisms and glacier sliding over the bedrock. Neither the past climate changes nor the present-day geographical situation are reliably known. Thus, the simplicity of the above model, with explicitly introduced parameters that have clear physical meaning, is its principal advantage and makes it a useful instrument in glaciological studies.

A schematic map of the Vostok lake vicinities adapted after Siegert and Ridley (1998) is presented in Figure 1a. The reference ice flowline passing through Vostok station and the ice-flow tube are depicted by the arrowed bold solid and dashed lines, respectively. They are drawn perpendicular to the surface elevation contours (Siegert and Ridley, 1998) for the grounded part of the ice sheet and after Siegert and others (2001) and Bell and others (2002) over the lake. The relative ice-flow tube width $H(s)$ vs distance s from Ridge B is shown in Figure 1b. The smoothed present-day ice-sheet thickness $\Delta_0(s)$ along the Vostok flowline also plotted in the figure is deduced from the airborne radio-echo sounding profile (Siegert and others, 2001) and the detailed geographic data (Bell and others, 2002; Tabacco and others, 2002; Studinger and others, 2003). The spatial distribution of the normalized mass balance $\bar{b}(s)$ is drawn in Figure 1b with account of the mass-balance enhancement factor 1.65 estimated by Jouzel and others (1993) for Ridge B at the location of the Dome B ice core marked as DB in Figure 1a. The shape of the curve is taken as similar to the smoothed accumulation-rate profile along the traverse to Vostok passing through sites B37, B78 and VK114 (see Fig. 1a), with ice accumulation rates measured by Lipenkov and others (1998). Although such a projecting procedure is rather schematic, the resulting normalized distribution $\bar{b}(s)$ compares in general to the spatial accumulation-rate changes which might be derived from tracing the internal radar layers along the Vostok ice flowline (Leysinger Vieli and others, 2004).

The values and a priori ranges of the basic model parameters considered in computations are given in Table 1. The present-day accumulation rate at Vostok was assumed on the basis of several studies (Barkov and Lipenkov, 1996; Ekaykin and others 2001, 2003), with the lower and upper bounds determined as the mean values over last 200 and 50 years, respectively. The ice densification and flow parameters are estimated and discussed in Salamatin (2000) and Barkov and others (2002). The exponential approximation of the snow–firn density profile (c_s and γ_s in Equation (4)) is additionally confirmed by the new data (Ekaykin and others, 2003).

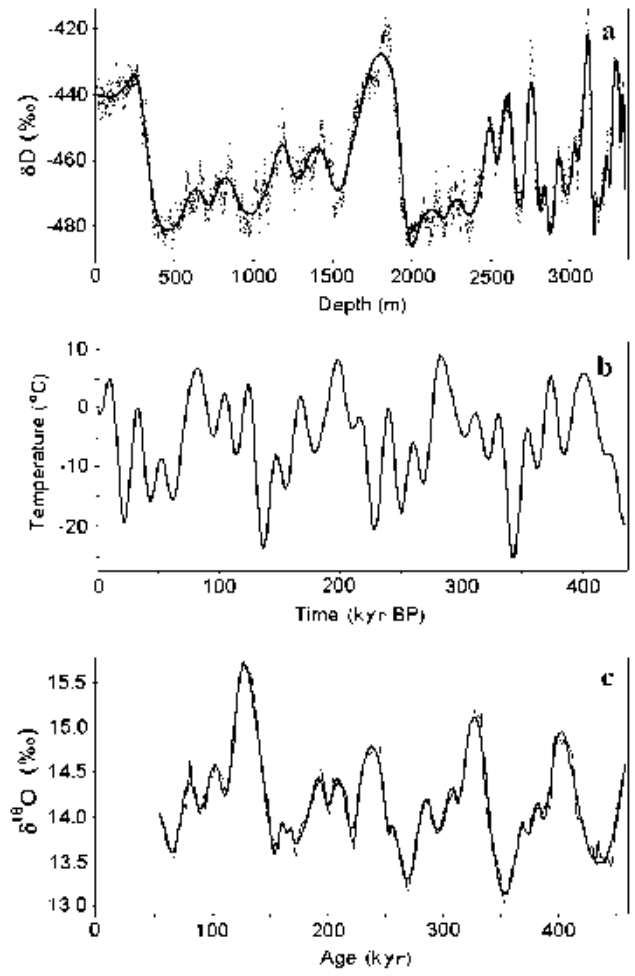

Fig. 2. Paleoclimatic signals used to constrain the ice-flow model and the simulated (glaciological) ice age–depth relationship at Vostok. (a) Vostok ice-core deuterium record (dots) and its parabolic spline approximation (solid line). (b) Geophysical metronome inferred from the borehole temperature profile at Vostok. (c) DH $\delta^{18}O$ record (thin line) and its parabolic spline approximation (bold line).

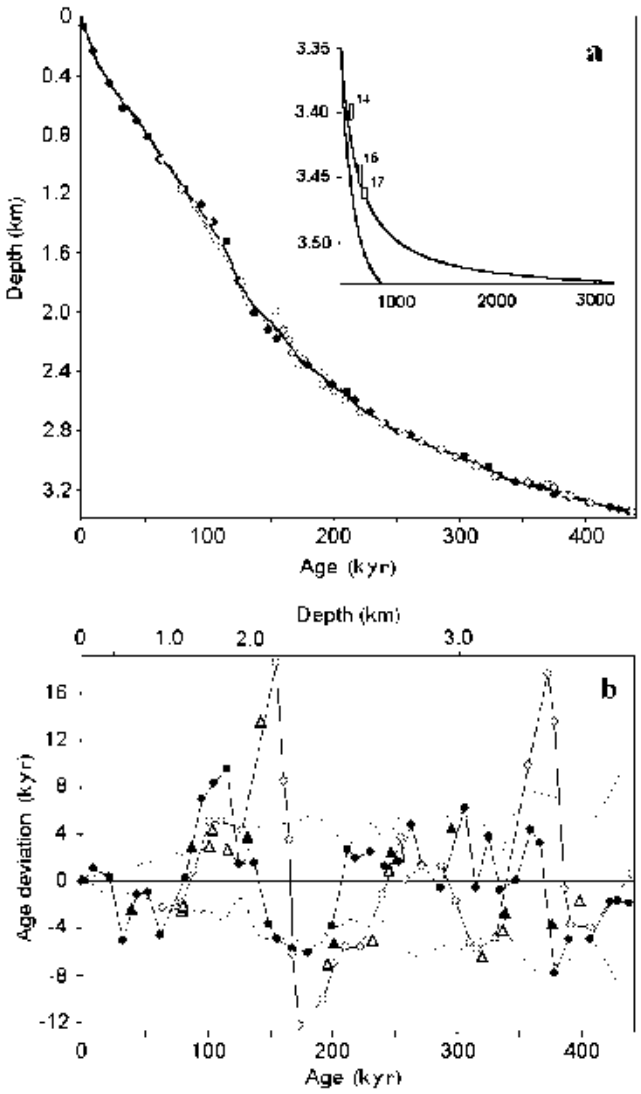

Fig. 3. Different ice age-datings at Vostok. (a) Best-fit glaciological time-scale (thin solid line) and average ice age–depth relationship (bold line) compared with GMTS (filled circles) and DHVTS (open circles) age–depth correlation points used for constraining the ice-flow model. The inset shows upper and lower extensions of the glaciological time-scale to 3530 m depth, 10 m above the boundary with the accreted lake ice. Rectangles and numbers are the climatic stages discerned in the Vostok dust concentration record. (b) The deviation of the linearly interpolated GMTS and DHVTS ages (filled and open circles, respectively) from a reference time-scale (zero line) chosen as the mathematical expectation (best fit) of the sampled chronologies at Vostok. Filled and open triangles are the respective control points from Parrenin and others (2001) and Landwehr and Winograd (2001). The dashed lines are the SD bounds of the age–depth curves selected through the Monte Carlo sampling procedure.

3. ICE-CORE AGES IMPORTED FROM PALEOCLIMATIC SIGNALS

Vostok ice age-dating procedures considered in this study are substantially based on the deuterium ice-core record (Petit and others, 1999) plotted in Figure 2a together with its parabolic spline approximation (Salamatin, 2000). The GMTS results directly from correlation of the smoothed isotopic signal with the geophysical metronome (Milankovich cycles of the local surface temperature variations) inferred from the deep borehole temperature profile at Vostok (Salamatin and others, 1998a, b; Salamatin, 2000). The metronome is presented in Figure 2b. The GMTS correlation pairs, ages and depths of the respective climatic events (peaks and troughs) identified in the metronomic and isotopic signals are depicted in Figure 3a by filled circles. It should be noted that the ice-core analysis (Petit and others, 1999) revealed some indications of ice-flow disturbances below 3310 m at Vostok. This reduces the confidence in identification and correlation of the two last extrema in the isotope record, although their ages display the right tendency to increase with depth. The eight orbital ice-age control points used in Parrenin and others (2001) are shown (filled triangles) in Figure 3b together with other age markers as deviations from a common reference time-scale explained below in section 4. They are in close agreement with linear interpolations between the GMTS correlation points: the age deviation is <1 kyr on average.

Next, we applied the parabolic spline approximation to the Devils Hole (DH) paleoclimatic record (Winograd and others, 1992) as plotted vs time in Figure 2c. The extrema in the Vostok deuterium–depth curve are now identified with the corresponding maxima and minima discerned in the

smoothed DH signal. Thus, another independent series of 31 DH age markers is transferred to the Vostok ice core (see open circles in Fig. 3a). These points are also presented in Figure 3b together with 12 age–depth pairs (open triangles) chosen by Landwehr and Winograd (2001) for importing the DH chronology. The standard deviation of the latter set of Vostok age estimates from the linear interpolations between the newly deduced correlations of the climatic events is about 1.6 kyr. Hence, the DH-to-Vostok time-scale (DHVTS) based on the spline representation of the DH isotope paleorecord is consistent with the earlier age–depth correlation established in Landwehr and Winograd (2001).

Remarkably, the mean difference between GMTS and DHVTS within the age interval of their overlap (60–430 kyr) is practically zero (~0.2 kyr). The periods of constant-sign deviations do not exceed several times 10^4 years. This indicates that there is no significant systematic (long-term) shift of one time-scale with respect to another. At the same time, the mean-square (standard) deviation (SD) is rather high, ~7.6 kyr, and maximum mismatches reach 10–15 kyr (see Fig. 3a and b). Cuffey and Vimeux (2001) give a good illustration of how sensitive the details of isotope paleorecords are to changes in their water-vapor sources and, hence, to their origins. In addition, the drift of snow-accumulation waves (megadunes) on the ice-sheet surface (Van der Veen and others, 1999) and post-depositional effects may also cause specific perturbations in ice-core isotopic records on time-scales of thousands of years, as revealed by Ekaykin and others (2002, 2003) and discussed by Waddington and others (2002) for shorter periods. The geophysical metronome, as a sum of Milankovich cycles, originally assumes a quasi-linear response of the Earth's climate to orbital forcing with fixed constant frequencies and phase shifts, disregarding 'climatic noise' and possible non-linearities (Salamatin and others, 1998b; Salamatin, 2000). Thus, the above estimates may be understood if the ages from two different series with statistically independent perturbations (errors) of 4–6 kyr are intercompared. These conclusions are important and allow us to use the GMTS and DHVTS age–depth correlation points to constrain the ice-flow model in the Vostok area on average, with minimum systematic errors in ice age predictions to a depth of 3350 m.

4. ICE-FLOW MODEL CONSTRAINTS AND GLACIOLOGICAL TIME-SCALE

Equations (1–4) were first validated on the best-guess time-scale simulated for the Vostok ice core by Parrenin and others (2001) with the use of the general 2-D model for Antarctic ice-sheet dynamics (Ritz, 1992). For an appropriate choice of parameters, the simplified model (1–4) reproduced the ice age–depth curve with accuracy no worse than 1.5 kyr. Such a close agreement and earlier applications of this approach for ice-core dating at Dome Fuji (Hondoh and others, 2002) and Vostok (Barkov and others, 2002) support the idea that Equations (1–3), being properly constrained, describe the ice age–depth distribution in an ice sheet on a macroscale level with an accuracy comparable to that of the thermomechanical 2-D and 3-D models. Approximations (1) and (2) and the smoothed geographic data in Figure 1 do not capture the fine spatial and temporal variations of the flow tube which will be a source of high-frequency noise in the simulated age–depth relation. These perturbations are not correlated with the ice age-dating errors introduced by use of the geophysical metronome or the DH paleoclimatic signal. Consequently, we expect that the modeled (glaciological) time-scale at Vostok, fitted to the two depth–age relationships of different origins (GMTS and DHVTS), might be considered as another source of ice age estimates with minimum systematic error, though containing independent short-term distortions.

Table 2. Estimates of the model tuning parameters deduced through the Monte Carlo sampling method for $\beta = 10$ ($\beta = 20$)

Parameter	Best fit	Mean	SD
Deuterium/inversion-temperature slope: C_T (‰ °C^{-1})	6.3	5.6	0.56
	(6.0)	(5.6)	(0.56)
Present-day ice accumulation rate: b_0 (cm a^{-1})	2.15	2.26	0.075
Shear-flow rate factor in the intermediate zone: σ_I	0.23	0.24	0.12
	(0.31)	(0.34)	(0.2)
Ice-sheet western grounding line: s_h (km)		275	–
Ridge B highlands boundary: s_h (km)		<25	–

Here we follow Parrenin and others (2001) and employ the inverse Monte Carlo sampling procedure (e.g. Mosegaard and Tarantola, 1995; Mosegaard, 1998) to study the sensitivity of the target function, the standard deviation of the glaciological time-scale from GMTS and DHVTS, to five tuning parameters: the present-day accumulation rate at Vostok, b_0; the deuterium-content/inversion-temperature temporal slope, C_T (or equally η_b/C_T); the location of the ice-sheet western grounding line at Vostok lake, s_l with $\sigma = 0$ for $s_0 > s > s_l$; the boundary of the Ridge B highlands, s_h with relatively high $\sigma \sim 0.5$–1.0 for $0 < s < s_h$; and the shear-flow rate factor upstream of the lake in the intermediate zone σ_I ($\sigma = \sigma_I$, $s_h < s < s_l$). The plausible a priori ranges for these values are given in Table 1. Several series of computational experiments were conducted to perform the resolution analyses with different combinations of the model parameters at different constraints. The best-fit estimates, obtained through the Monte Carlo method and discussed below, are summarized in Table 2.

Preliminary tests showed unequal uncertainty levels of GMTS and DHVTS, with the latter age fluctuations around the fitted model predictions 1.4–1.7 times higher than those of GMTS. The respective absolute values of the 'Gaussian noise' SD assumed in the likelihood function of the Metropolis algorithm were estimated as 4.7–4.3 and 6.6–7.4 kyr. Although these uncertainties include the modeling errors, they are close to the claimed accuracies of GMTS and the DH age dating. In each computational experiment, about 10^3–(5×10^3) uncorrelated chronologies were selected at 35% level of acceptance by the Monte Carlo scheme. Depending on a frequency of selection related to the number of inferable parameters and assumed ranges of their variation, the total number of tested time-scales was 10^5–10^6.

In general, the resolution analysis performed by means of the random-walk sampling shows that the resulting posterior probability density in the space of the ice-flow model parameters is not unimodal and has an extended domain of

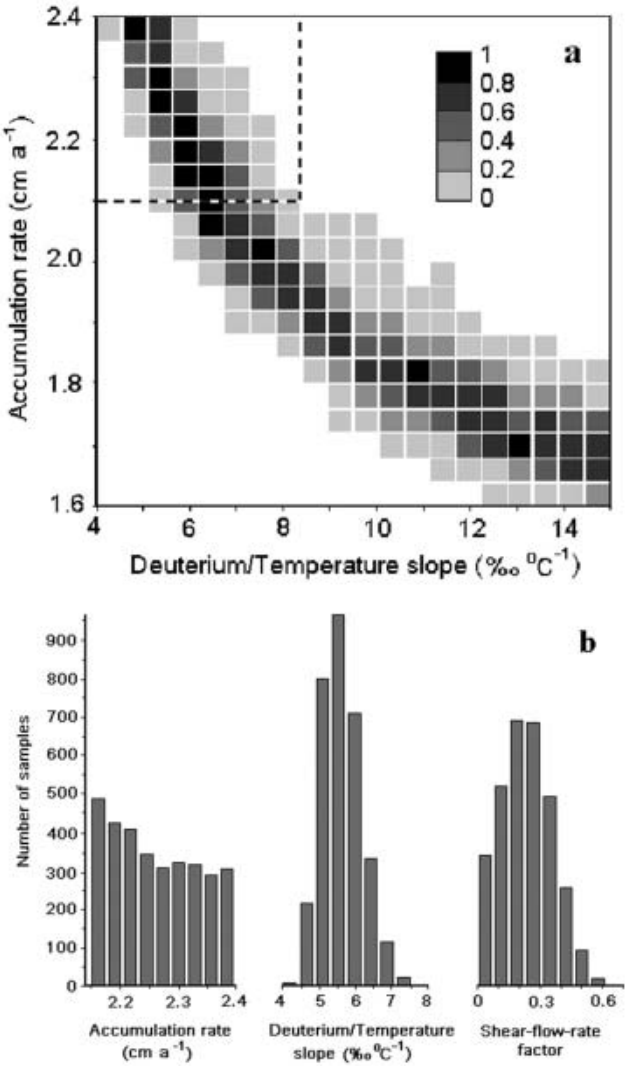

Fig. 4. The a posteriori information on the ice-flow model parameters deduced through the Monte Carlo sampling procedure. (a) A map of the normalized sampling probability density on the b_0–C_T phase plain. (b) The histograms of the three principal model parameters: present-day accumulation rate b_0 at Vostok, deuterium/inversion-temperature slope C_T, and shear-flow rate factor σ_l explored in the bold-dashed outlined rectangle domain in (a).

global maximum. This means that feasible variations of some parameters can be counterbalanced by a priori accepted changes in the others. Only additional restricting information on the model parameters can lead to a more definite estimation. Nevertheless, all best-fit chronologies found in different computational series are practically indistinguishable and fell within 5.9 ± 0.3 kyr limits of the standard deviation from the GMTS and DHVTS age markers. This implies that the model (1–4) is sufficiently flexible and the simulated depth–age relationship can be uniquely constrained by the available chronological information at plausible values of the tuning parameters. The thin solid line in Figure 3a depicts the best-fit glaciological time-scale. It converges to the mathematical expectation of the sampled (selected) age–depth curves. Deviations of the GMTS and DHVTS ages from the statistical mean, best-fit, ages (zero line) are plotted in Figure 3b. The dashed lines are the SD bounds of the tested chronologies. Since GMTS and DHVTS are used as model constraints, a certain apparent similarity of their fluctuations around the glaciological time-scale in Figure 3b should be assigned mainly to the short-term details missed in the modeled age–depth curve, and not to the systematic statistically correlated errors between the time-scales themselves.

With this result, let us discuss a posteriori information on the model parameters deduced through the Monte Carlo procedure. First, the deuterium/inversion-temperature slope C_T enters Equations (2) as a ratio to η_b, and its estimates automatically include all errors of the latter factor (Ritz, 1992) as well as the general uncertainties of the assumed Robin's (1977) geographic relationship. Hence, the obtained values of C_T cannot be directly interpreted in terms of the transfer function between the ice-core isotope content and inversion temperature. Furthermore, as clearly seen from Equation (3), for the major part of the ice sheet (for $\zeta > 0.1$–0.2) the ice age–depth distribution is mainly controlled by the ratio $\sigma/(\beta+1)$, and any change in β correspondingly influences the inferable values of σ. Therefore, in the basic series of computations, we fixed $\beta = 10$ in accordance with Salamatin and Ritz (1996).

Initial random-walk sampling over the complete set of five model parameters b_0, C_T, σ_l, s_l and s_h within the limits given in Table 1 revealed an important tendency that for any σ in the Ridge B highland area ($0 < s < s_h$) the optimal position of s_h was shifted towards 20–25 km distance from the ice divide, and the ice age predictions above 3350 m depth near Vostok station became insensitive to the σ values. Correspondingly, in further computational experiments we assumed $s_h = 20$ km. Next, extremely low sensitivity of the modeled glaciological time-scale was observed with respect to the grounding-line location s_l, with a very weak maximum of the sampling probability around 50–60 km from Vostok, in full agreement with Bell and others (2002). Thus, s_l was fixed as 275 km from Ridge B. After that, the reconnaissance resolution analysis was performed in the space of the three parameters (b_0, C_T and σ_l) within much wider ranges than the a priori bounds set in Table 1, for b_0 from 1.4 to 2.4 cm a^{-1} and for C_T from 4 to 15‰ °C^{-1}. A 2-D map of the normalized probability density sampled by the Monte Carlo method on the b_0–C_T phase plane is plotted in Figure 4a. It clearly shows that only the values of $C_T \sim 5$–7‰ °C^{-1} are consistent with the a priori estimates of $b_0 \sim 2.15$–2.4 cm a^{-1} (see the bold-dashed outlined rectangle domain in Fig. 4a). The best fit becomes insensitive to the deuterium/temperature slope and shifts to unreasonably low values of the present-day accumulation rates $B_0 \sim 1.6$–1.9 cm a^{-1} for $C_T \sim 8$–15‰ °C^{-1}. As can easily be understood, this corresponds to the limiting case of Equations (2) at $C_T \to \infty$ when temporal variations of the accumulation rate are suppressed and B_0 tends to its long-term average value ($\sim$1.3–1.5 cm a^{-1}). Finally, the localized area of the feasible b_0 and C_T variations was additionally explored with the random-walk sampling. As might be expected, the inverse procedure revealed in this case a nearly uniform distribution of the sampling probability density vs b_0, a 'sharp' unimodal histogram for C_T and a clearly resolved maximum in the histogram for σ_l. All three distribution functions are presented in Figure 4b. The corresponding estimates of the model parameters are given in Table 2. The best fit was found at a standard deviation of the glaciological time-scale from GMTS and DHVTS (the target function value) of about 5.8 kyr. The inferred values of $C_T \approx 5.6 \pm 0.6$‰ °C^{-1} agree with previous results based

on the borehole temperature analysis (Salamatin and others, 1998b) and preliminary simulations of the ice-sheet dynamics (Barkov and others, 2002). This slope determines a deuterium-ratio–inversion-temperature relationship, which falls exactly midway between the bounds reconstructed by the inverse procedure in Parrenin and others (2001). The use of the correction factor 4.8 for the water-isotopic composition in the first of Equations (2), instead of 8, reduces the above estimates of C_T by approximately 6% without influencing the ice dating. The best-fit present-day accumulation rate is found at its lower bound, $2.15\,\mathrm{cm\,a^{-1}}$, and matches with the mean value, $2.2 \pm 0.03\,\mathrm{cm\,a^{-1}}$, calculated for the recent 200 years from the depths of the Tambora (Indonesia) eruption layer measured at Vostok in nine shallow boreholes and deep pits (Ekaykin and others, 2003). Rather low values of $\sigma_l \geq 0.24 \pm 0.1$ are indicative of intense sliding over the glacier bed and/or soft-ice shear zone development in the basal layer. The former peculiarity could be the model artifact attributable to the substitution of the smoothed bedrock profile for the natural subglacial relief with high undulations (see Siegert and others, 2001), while the latter is a realistic phenomenon observed in Vostok ice cores (Lipenkov and others, 2000) and simulated by Salamatin and Malikova (2000). All these findings remained generally unchanged for $\beta = 20$ (see Table 2) at similar estimates of the model parameters, except for the expected increase in the shear-flow rate factor: $\sigma_l \approx 0.34 \pm 0.2$.

5. AVERAGE TIME-SCALE: DISCUSSION

The three depth–age relationships introduced and compared in the previous sections are uniformly consistent with each other to the maximum depth, 3350 m, of the Vostok ice core. The errors in these primary, basic time-scales differ in magnitude and by origin. On average, the uncertainty level of age dating can be predicted with a $\sqrt{2}$ reduction compared to the standard deviation of the best-fit (glaciological) time-scale from GMTS and DHVTS: that is, not higher than 4.2 kyr. However, the latter estimate and the statistical validity of ice-core dating might be additionally improved if the difference in error levels is taken into account. For example, SD between the best-fit time-scale and GMTS is 4.3–4.7 kyr. Hence, the average accuracy of their mean ages is about 3.0–3.3 kyr. Accordingly, we assume that each of the three basic depth–age relationships has its own uncertainty level, and iteratively calculate the weighted mean time-scale using the running averaging procedure over a 4 kyr interval comparable with the average error level. The weights are taken inversely proportional to standard deviations of the basic chronologies from the resulting smoothed average curve. This condition yields converged normalized weighting coefficients of 0.44, 0.38 and 0.18 for the best-fit glaciological time-scale, GMTS and DHVTS, respectively, with the corresponding standard deviations from the mean ages equal to 2.2, 2.6 and 5.6 kyr. The latter estimates characterize the quality of different sources of chronological information and reveal the higher statistical validity (the lower error level) of the properly constrained glaciological time-scale. The bold line in Figure 3a shows the average time-scale. The deviations of the three basic time-scales from the average age–depth curve (zero line) are plotted in Figure 5a. The dot-dashed lines in the figure are the total standard error bounds of ±3.6 kyr which correspond to the upper estimate of the age

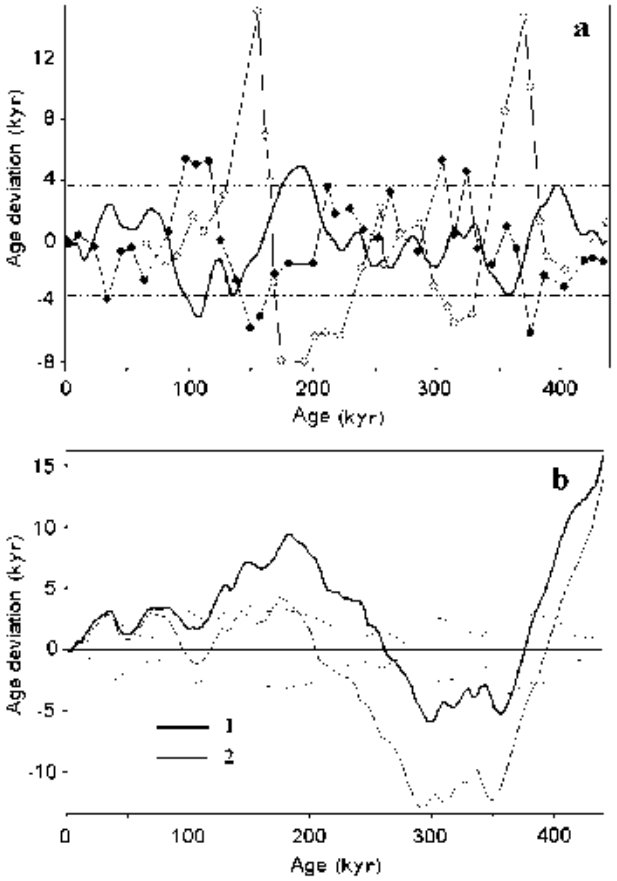

Fig. 5. Comparison of the average time-scale developed for the Vostok ice core with other time-scales of different origins. (a) The deviation of the three Vostok age–depth relationships, i.e. GMTS (linearly interpolated filled circles), DHVTS (linearly interpolated open circles) and the best-fit glaciological time-scale (bold line) from the averaged time-scale (zero line). The dot-dashed lines show the standard error bounds of the mean ages. (b) Deviation of the best-guess time-scale (Parrenin and others 2001) and GT-4 (Petit and others, 1999) from the average time-scale: bold (1) and thin (2) curves, respectively. Dotted lines are the running weighted mean SD bounds of ice ages from Table 3.

uncertainty. Actually, the deduced error level of the best-fit glaciological time-scale, ±2.2 kyr, i.e. the weighted mean SD of all three chronologies, is thought to be a more reliable measure of the accuracy of the newly developed time-scale. The average age–depth relationship is presented in Table 3 together with the running weighted mean SD (errors) also shown in Figure 5b by dashed lines. Because of the ice-flow disturbances, the actual errors below 3310 m may be higher, and question marks follow the respective SD estimates in Table 3. The average time-scale has also been substituted into Equations (2) to calculate the isotopic content of precipitation vs time and, thus, is additionally fitted through iterations.

Both Figure 5 and Table 3 show non-uniform distribution of errors vs depth and age. The age uncertainties range from 0.25 to 3–4 kyr at maximum. Obviously, the highest errors are located around 110, 140, 180 and 360 kyr (1500, 2000, 2350 and 3170 m), mainly where the maximum mismatch between the Vostok and DH isotopic records and/or their chronostratigraphies is observed (see Figs 3b and 5a). In all these cases, the best-fit glaciological depth–age relationship

Table 3. Average age–depth relationship for Vostok ice core and its theoretical extension to the boundary with the accreted lake ice

Depth m	Age kyr	SD kyr	Depth m	Age kyr	SD kyr
0.0	0	0.0	2773.4	244	0.8
110.0	4	0.2	2794.3	248	1.0
204.5	8	0.4	2811.4	252	1.1
288.3	12	0.7	2826.5	256	1.3
356.7	16	0.8	2840.8	260	1.5
413.2	20	0.6	2855.3	264	1.3
465.6	24	0.9	2870.2	268	0.8
517.8	28	1.6	2884.2	272	0.4
568.8	32	2.2	2897.8	276	0.3
613.9	36	2.4	2911.9	280	0.4
654.4	40	2.0	2926.5	284	0.4
696.4	44	1.2	2940.4	288	0.7
742.5	48	0.8	2953.5	292	1.4
793.5	52	0.7	2965.9	296	2.2
849.3	56	0.9	2977.9	300	2.4
905.9	60	1.4	2991.1	304	1.9
956.3	64	1.7	3007.5	308	1.4
1001.9	68	1.6	3025.1	312	1.3
1047.7	72	1.4	3040.0	316	1.8
1095.6	76	1.0	3052.6	320	2.1
1146.6	80	0.7	3066.9	324	1.9
1197.2	84	1.2	3085.4	328	1.5
1244.4	88	2.2	3105.1	332	1.2
1288.7	92	2.8	3122.6	336	0.9
1334.9	96	3.0	3136.8	340	1.3
1386.3	100	3.2	3147.5	344	2.0
1441.0	104	3.5	3155.2	348	2.6
1495.1	108	3.7	3161.5	352	3.1
1547.8	112	3.4	3168.1	356	3.5
1609.2	116	2.5	3175.4	360	3.4
1686.7	120	1.4	3183.5	364	3.0
1772.0	124	1.2	3193.0	368	2.5
1850.3	128	2.0	3204.1	372	2.3
1914.2	132	3.0	3215.6	376	2.5
1964.9	136	3.8	3226.2	380	3.0
2004.3	140	4.0	3235.9	384	2.9
2038.7	144	3.7	3245.2	388	2.6
2072.1	148	3.4	3254.6	392	2.6
2104.7	152	3.3	3264.3	396	2.6
2139.3	156	3.1	3274.7	400	2.4
2176.5	160	2.7	3285.3	404	2.1
2215.1	164	2.4	3295.4	408	1.7
2255.0	168	2.4	3304.8	412	1.2
2291.1	172	2.7	3313.5	416	0.9(?)
2321.2	176	3.0	3321.2	420	0.8(?)
2348.8	180	3.3	3328.4	424	0.9(?)
2375.5	184	3.5	3335.6	428	0.8(?)
2402.3	188	3.4	3342.5	432	0.9(?)
2429.6	192	3.2	3348.1	436	1.0(?)
2457.7	196	2.9	3350.0	438	1.1(?)
2485.8	200	2.4	Extrapolated time-scale		
2512.9	204	2.2	3368	457	15
2538.9	208	2.1	3386	477	19
2567.7	212	1.9	3404	500	24
2601.3	216	1.8	3422	528	33
2633.0	220	1.8	3440	564	44
2658.5	224	1.8	3458	611	63
2680.4	228	1.7	3476	680	96
2701.8	232	1.4	3494	790	141
2724.5	236	1.0	3512	1019	319
2749.3	240	0.7	3530	1956	1118

and GMTS agree with the average time-scale within the standard uncertainty bounds, and only the ages imported from the DH paleosignal display abrupt fluctuations with 2–2.5 higher amplitudes. To track such extreme variations of DHVTS by the ice-flow model, in simulations, we would need accumulation rates at least two times higher (or lower) than those predicted by the first of Equations (2), continuously during 25–50 kyr intervals. This seems unrealistic and most likely is due to the different origins of the Vostok and DH isotopic records.

In Figure 5b the average time-scale is compared to GT-4 and the best-guess time-scale developed for Vostok ice cores by Petit and others (1999) and Parrenin and others (2001). Both age–depth curves significantly, although within their accuracy limits, deviate from the average time-scale (zero line in Fig. 5b). Such a discrepancy may be a consequence of overtuning the ice flow in these other models to a limited (statistically non-representative) number of specific control points (e.g. see Fig. 3b).

We can now estimate the ice age at Vostok below 3350 m, although because of the ice-flow disturbances below 3310 m (Petit and others, 1999) such an attempt may be just a theoretical exercise. However, recent studies of the deepest part of the Vostok glacier ice (Simões and others, 2002) showed that the glacial stages 14 and 16 are still distinctly discernible in the dust concentration record within the depth intervals 3393–3405 and 3440–3455 m, respectively, and most likely that interglacial stage 17 covers the depth range 3457–3466 m. This suggests that the ice, at least to 3470 m depth, has undergone only local perturbations. Hence, an extension of the time-scale toward the boundary with the accreted lake ice, to a depth of 3540 m, can provide an estimation of possible maximum variations of ice ages and the statistically expected age–depth distribution.

First we calculated the long-term average accumulation rate, 1.4 cm a^{-1}, at Vostok over four climatic cycles, using Equation (2) with the best-fit estimates of b_0 and C_T (see Table 2). Then, the best-fit glaciological time-scale has been continued in our simulations to 3530 m depth, with the averaged accumulation rate assumed for the paleoclimatic history before 430 kyr BP. Predicted ice ages in the bottom part depend on the Ridge B highland boundary S_h and the shear-flow rate factor σ_h in this area ($0 < s < s_h$), increasing with s_h and σ_h. Parameter σ_h in the cold vicinities of Ridge B cannot be lower than σ_1 in the intermediate zone. Consequently, only the limiting values of $\sigma_h = \sigma_1$ and $\sigma_h = 1$ have been tested in simulations at the lower (best-fit) and upper values of $s_h = 20$ and 80 km, respectively. The latter estimate for s_h is the maximum geographic constraint (see Fig. 1b). This was confirmed in preliminary computational experiments which showed low sensitivity of the best-fit glaciological time-scale (~0.5 kyr) to s_h within the above range and revealed an exponential increase in its standard deviation from GMTS and DHVTS from 6 to 17 kyr for higher s_h values from 80 to 200 km. The computed respective lower and upper age bounds plotted in the inset in Figure 3a are obtained with the apparent creep index $\beta = 10$ and for β linearly decreasing from 10 to 1 upstream from $s_h = 80$ km. Their arithmetic mean agrees with the average time-scale below 3310 m with an accuracy of about 1 kyr and continues it at the end of Table 3. The error estimates are the mean age deviations from the simulated bounds plus additional standard errors caused by averaging the past accumulation rates before 430 kyr BP and estimated

to be ~6 kyr. The maximum ice age at 3530 m could reach 1960 ± 1120 kyr, provided that the basal ice flow has not been disturbed. Higher values of $\beta > 10$ do not change the age estimates. The depth ranges of the stages 14, 16 and 17 suppositionally observed in the dust concentration record (Simões and others, 2002) and their durations estimated in Bassinot and others (1994) are shown as rectangles in the inset in Figure 3a and are in agreement with the theoretical upper bound.

6. CONCLUSION

Three different approaches to ice-core age dating are employed to develop an average age–depth relationship at Vostok. Firstly, the GMTS, extended in Salamatin and others (1998a) and Salamatin (2000) to the maximum depth 3350 m of the Vostok ice-core isotope record covering four interglaciations, is used as a so-called orbitally tuned chronology. It is based on correlation of the isotopic temperature signal with the geophysical metronome Milankovich components of past local surface temperature variations inferred from the borehole temperature profile. Another paleotemperature proxy signal spanning >500 000 years is available from the calcite core (DH-11) in Devils Hole (Winograd and others, 1992, 1997). The principal advantage of this $\delta^{18}O$ record is that the dense vein calcite provides a material for direct uranium-series dating (Ludwig and others, 1992). The correlation of the Vostok ice-core deuterium–depth signal with the DH record yields a second, independent, time-scale (DHVTS). Ice-flow modeling also becomes a useful tool for ice age prediction if a priori chronological information is used to constrain the model parameters. Here we base our study on a simplified 2-D approach to ice flowline simulations as described in Salamatin and Ritz (1996) and Hondoh and others (2002). Consequently, the modeled (glaciological) time-scale at Vostok fitted to the GMTS and DHVTS represents a third source of ice age estimates and incorporates the principal laws of ice-sheet dynamics into the ice-core dating procedure. The inverse Monte Carlo sampling method proves to be especially helpful for constraining the accumulation-rate reconstruction and ice-flow modeling to find the best-fit glaciological time-scale matched with the two other chronologies (see Table 2). General uncertainties of the above age estimates vary from 2 to 6 kyr on average and reach 6–15 kyr at maximum. Whatever the causes of these discrepancies might be, they are thought to be of different origins, with statistically independent errors. Thus, the average time-scale for the Vostok ice core down to 3350 m depth is deduced consistent with all three dating procedures within the standard deviation limits of ±3.6 kyr. The estimate of the actual accuracy of the developed average age–depth relationship should take into account the different error levels of the primary basic time-scales and is predicted as ±2.2 kyr on average. The constrained ice-sheet flow model allows, at least theoretically, extrapolation of the mean ice age–depth curve to the boundary with the accreted lake ice where the glacier-ice age at 3530 m depth may reach (or even exceed) ~2000 kyr.

ACKNOWLEDGEMENTS

The authors are grateful to J. M. Landwehr and I. J. Winograd for DH data and useful comments. F. Parennin provided data and explanations of his Vostok age simulations, and valuable suggestions. We thank M. J. Siegert and G. J.-M. C. Leysinger Vieli for help with geographical data. We also acknowledge fruitful discussions with participants in the 2002 meeting on 'Russian–French Collaboration on Vostok Ice Cores' in St Petersburg. We thank two anonymous reviewers and T. van Ommen for editorial assistance. This study has been supported through the Joint Research INTAS (International Association for the Promotion of Cooperation with Scientists from the Independent States of the Former Soviet Union) Project 'A connection of the isotope composition of recent snow in central Antarctica (Vostok Station) with meteorological and climatic conditions, as related to interpretation of ice-core records' (INTAS-2001-2268).

REFERENCES

Barkov, N. I. and V. Ya. Lipenkov. 1996. Nakopleniye snega v rayone stantsii Vostok, Antarktida, v 1970–1992 gg [Snow accumulation at Vostok station, Antarctica, in 1970–1992]. *Mater. Glyatsiol. Issled./Data Glaciol. Stud.,* **80**, 87–88. [In Russian with English summary.]

Barkov, N. I., R. N. Vostretsov, V. Ya. Lipenkov and A. N. Salamatin. 2002. Kolebaniya temperatury vozdukha i osadkov v rayone stantsii Vostok na protyazhenii chetyryeh klimaticheskih tsyklov za posledniye 420 tys. let [Air temperature and precipitation variations in Vostok station area through four climatic cycles during recent 420 kyears]. *Arktika i Antarktika,* **1**(35), 82–97. [In Russian with English summary.]

Bassinot, F. C., L. Lebeyrie, E. Vincent, X. Quidelleur, N. J. Shackleton and Y. Lancelot. 1994. The astronomical theory of climate and the age of the Brunhes–Matuyama magnetic reversal. *Earth Planet. Sci. Lett.,* **126**(1–3), 91–108.

Bell, R. E., M. Studinger, A. A. Tikku, G. K. C. Clarke, M. M. Gutner and C. Meertens. 2002. Origin and fate of Lake Vostok water frozen to the base of the East Antarctic ice sheet. *Nature,* **416**(6878), 307–310.

Cuffey, K. M. and F. Vimeux. 2001. Covariation of carbon dioxide and temperature from the Vostok ice core after deuterium-excess correction. *Nature,* **412**(6846), 523–527.

Ekaykin, A. A., V. Ya. Lipenkov, N. I. Barkov, J. R. Petit and V. Masson. 2001. Izotopniy sostav poverhnostnogo sloya snezhnoy tolschi v rayone stantsii Vostok, Tsentral'naya Antarktida [Isotopic composition of upper part of snow layer at Vostok station area, central Antarctica]. *Mater. Glyatsiol. Issled./Data Glaciol. Stud.,* **90**, 69–79. [In Russian with English summary.]

Ekaykin, A. A., V. Ya. Lipenkov, N. I. Barkov, J. R. Petit and V. Masson-Delmotte. 2002. Spatial and temporal variability in isotope composition of recent snow in the vicinity of Vostok station, Antarctica: implications for ice-core record interpretation. *Ann. Glaciol.,* **35**, 181–186.

Ekaykin, A. A., V. Ya. Lipenkov, J. R. Petit and V. Masson-Delmotte. 2003. 50-letnii tsikl v izmeneniyah akkumulyatsii i izotopnogo sostava snega na stantsii Vostok [50-year cycle in variations of accumulation rate and isotopic composition of snow at Vostok station]. *Mater. Glyatsiol. Issled./Data Glaciol. Stud.,* **94**, 163–173. [In Russian with English summary.]

Hondoh, T., H. Shoji, O. Watanabe, A. N. Salamatin and V. Ya Lipenkov. 2002. Depth–age and temperature prediction at Dome Fuji station, East Antarctica. *Ann. Glaciol.,* **35**, 384–390.

Jouzel, J. *and 16 others*. 1993. Extending the Vostok ice-core record of palaeoclimate to the penultimate glacial period. *Nature,* **364**(6436), 407–412.

Jouzel, J. *and 6 others*. 2003. Magnitude of isotope/temperature scaling for interpretation of central Antarctic ice cores. *J. Geophys. Res.,* **108**(D12), 4361–4370. (10.1029/2002JD002677.)

Landwehr, J. M. and I. J. Winograd. 2001. Dating the Vostok record by importing the Devils Hole chronology. *J. Geophys. Res.,* **106**(D23), 31,837–31,851.

Leysinger Vieli, G. J.-M. C., M. J. Siegert and A. J. Payne. 2004. Reconstructing ice-sheet accumulation rates at Ridge B, East Antarctica. *Ann. Glaciol.,* **39** (see paper in this volume).

Lipenkov, V. Ya., A. A. Ekaykin, N. I. Barkov and M. Pourchet. 1998. O svyazi plotnosti poverkhnostnogo sloya snega v Antarktide so skorost'yu vetra [On the connection between density of surface ice layer in Antarctica with wind velocity]. *Mater. Glyatsiol. Issled./Data Glaciol. Stud.,* **85**, 148–158. [In Russian with English abstract.]

Lipenkov, V. Ya., N. I. Barkov and A. N. Salamatin. 2000. Istoriya klimata i oledeneniya Antarktidy po rezul'tatam izucheniya ledanogo kerna so stantsii Vostok [The history of climate and glaciation of Antarctica from results of the ice core study at Vostok station]. *Probl. Arkt. Antarkt.,* **72**, 197–236. [In Russian with English abstract.]

Lliboutry, L. 1979. A critical review of analytical approximate solutions for steady state velocities and temperatures in cold ice sheets. *Z. Gletscherkd. Glazialgeol.,* **15**(2), 135–148.

Ludwig, K. R. *and 6 others*. 1992. Mass-spectrometric ^{230}Th-^{234}U-^{238}U dating of the Devils Hole calcite vein. *Science,* **258**(5080), 284–287.

Mosegaard, K. 1998. Resolution analysis of general inverse problems through inverse Monte Carlo sampling. *Inverse Problems,* **14**(1), 405–426.

Mosegaard, K. and A. Tarantola. 1995. Monte Carlo sampling of solutions to inverse problems. *J. Geophys. Res.,* **100**(B7), 12,431–12,447.

Parrenin, F., J. Jouzel, C. Waelbroeck, C. Ritz and J.-M. Barnola. 2001. Dating the Vostok ice core by inverse method. *J. Geophys. Res.,* **106**(D23), 31,853–31,861.

Petit, J.-R. *and 18 others*. 1999. Climate and atmospheric history of the past 420,000 years from the Vostok ice core, Antarctica. *Nature,* **399**(6735), 429–436.

Ritz, C. 1989. Interpretation of the temperature profile measured at Vostok, East Antarctica. *Ann. Glaciol.,* **12**, 138–144.

Ritz, C. 1992. Un modèle thermo-mecanique d'évolution pour le bassin glaciaire Antarctique Vostok–glacier Byrd: sensibilité aux valeurs des paramètres mal connus. (Thèse de doctorat d'état, Université Joseph Fourier – Grenoble I.)

Ritz, C., V. Rommelaere and C. Dumas. 2001. Modeling the evolution of Antarctic ice sheet over the last 420,000 years: implications for the altitude changes in the Vostok region. *J. Geophys. Res.,* **106**(D23), 31,943–31,964.

Robin, G. de Q. 1977. Ice cores and climatic change. *Philos. Trans. R. Soc. London, Ser. B,* **280**(972), 143–168.

Salamatin, A. N. 2000. Paleoclimatic reconstructions based on borehole temperature measurements in ice sheets. Possibilities and limitations. *In* Hondoh, T., *ed. Physics of ice core records*. Sapporo, Hokkaido University Press, 243–282.

Salamatin, A. N. and D. R. Malikova. 2000. Structural dynamics of an ice sheet in changing climate. *Mater. Glyatsiol. Issled./Data Glaciol. Stud.,* **89**, 112–128.

Salamatin, A. N. and C. Ritz. 1996. A simplified multi-scale model for predicting climatic variations of the ice-sheet surface elevation in central Antarctica. *Ann. Glaciol.,* **23**, 28–35.

Salamatin, A. N., R. N. Vostretsov, J.-R. Petit, V. Ya. Lipenkov and N. I. Barkov. 1998a. Geophysical and palaeoclimatic implications of the stacked temperature profile from the deep borehole at Vostok station, Antarctica. *Mater. Glyatsiol. Issled./Data Glaciol. Stud.,* **85**, 233–240. [In English and Russian, parallel text.]

Salamatin, A. N., V. Ya. Lipenkov, N. I. Barkov, J. Jouzel, J.-R. Petit and D. Raynaud. 1998b. Ice core age dating and paleothermometer calibration based on isotope and temperature profiles from deep boreholes at Vostok Station (East Antarctica). *J. Geophys. Res.,* **103**(D8), 8963–8977.

Siegert, M. J. and J. K. Ridley. 1998. An analysis of the ice-sheet surface and subsurface topography above the Vostok Station subglacial lake, central East Antarctica. *J. Geophys. Res.,* **103**(B5), 10,195–10,207.

Siegert, M. J. *and 6 others*. 2001. Physical, chemical and biological processes in Lake Vostok and other Antarctic subglacial lakes. *Nature,* **414**(6864), 603–609.

Simões, J. C. *and 7 others*. 2002. Evidence of glacial flour in the deepest 89 m of the Vostok ice core. *Ann. Glaciol.,* **35**, 340–346.

Sowers, T. *and 7 others*. 1993. A 135,000-year Vostok–SPECMAP common temporal framework. *Paleoceanography,* **8**(6), 737–766.

Studinger, M. *and 11 others*. 2003. Ice cover, landscape setting, and geological framework of Lake Vostok, East Antarctica. *Earth Planet. Sci. Lett.,* **205**(3–4), 195–210.

Tabacco, I. E., C. Bianchi, A. Zirizzotti, E. Zuccheretti, A. Forieri and A. Della Vedova. 2002. Airborne radar survey above Vostok region, east-central Antarctica: ice thickness and Lake Vostok geometry. *J. Glaciol.,* **48**(160), 62–69.

Van der Veen, C. J., E. Mosley-Thompson, A. Gow and B. G. Mark. 1999. Accumulation at South Pole: comparison of two 900-year records. *J. Geophys. Res.,* **104**(D24), 31,067–31,076.

Waddington, E. D., E. J. Steig and T. A. Neumann. 2002. Using characteristic times to assess whether stable isotopes in polar snow can be reversibly deposited. *Ann. Glaciol.,* **35**, 118–124.

Winograd, I. J. *and 7 others*. 1992. Continuous 500,000 year climate record from vein calcite in Devils Hole, Nevada. *Science,* **258**(5080), 255–260.

Winograd, I. J., J. M. Landwehr, K. R. Ludwig, T. B. Coplen and A. C. Riggs. 1997. Duration and structure of the past four interglaciations. *Quat. Res.,* **48**(2), 141–154.